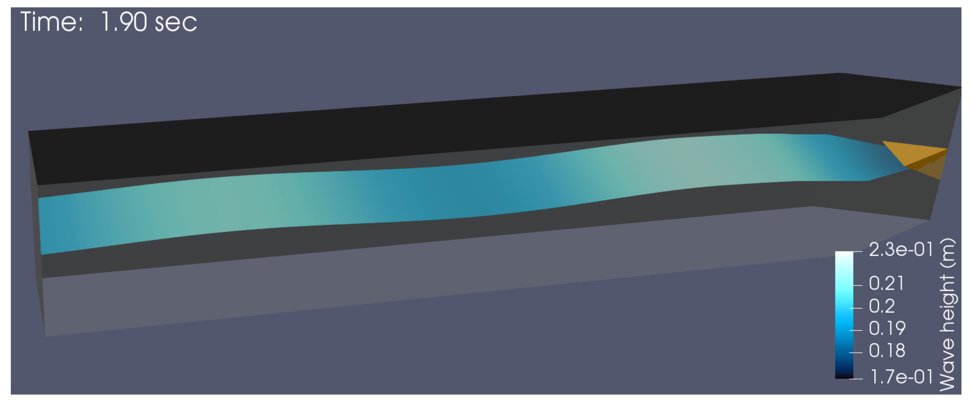

Rogue-wave-energy: wave-to-wire mathematical modelling

Onno Bokhove, School of Mathematics, University of Leeds, Leeds, UK –o.bokhove@leeds.ac.uk

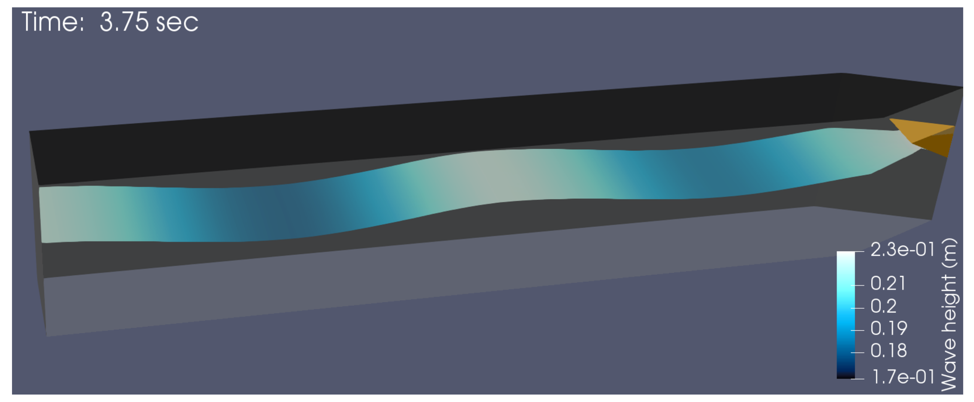

1. Objectives

A novel wave-energy device design [1,2] will be presented based on the following features: (i) an electro-magnetic generator based on cylindrical magnets moving through induction wires around a cylindrical tube, like in the IP wave-buoy, (ii) a convergence in a breakwater to amplify the incoming waves, like in the TapChan device, and (iii) a wave-activated buoy with magnets attached, like in the Berkeley wedge, constrained to move in a slight arc or in a rectilinear manner. Its workings have been demonstrated in a first, operating proof-of-principle.

3. Mathematical model

A monolithic mathematical model is established by coupling the three variational principles for the **hydrodynamic wave motion**, using the potential-flow approximation, the constrained wave-activated **buoy motion**, and the **electro-magnetic generator** together into one grand variational principle [1,2]. Resistive losses in the electrical circuit and the energy harvested in the (parallel LED) loads are subsequently added to the dynamics. The fully coupled system reads –for details see [1,2]:

$$\delta D : \partial_t \phi + \frac{1}{2}|\nabla \phi|^2 + g(z - H_0) + p = 0 \tag{1a}$$

$$\delta \phi : \partial_t D + \nabla \cdot (D \nabla \phi) = 0, \quad \delta p: \ D = 1 \tag{1b}$$

$$\delta \lambda : h - h_b = 0 \text{ buoy is tetrahedron at: } y > y_b(x,t), \quad z = h_b(x, y; Z(t)) = Z(t) - H_k - \tan\alpha\,(y - L_y) \tag{1c}$$

$$\delta \phi_s : \partial_t h + \nabla \phi \cdot \nabla h = \partial_z \phi \text{ at } z = h(x,y,t) \tag{1d}$$

$$\delta h : \quad \partial_t \phi + \frac{1}{2}|\nabla \phi|^2 + g(h - H_0) + \underline{\lambda \Theta (y - y_b(x,y,t))} = 0 \text{ at } z = h(x,y,t) \tag{1e}$$

$$\delta \phi_R : \dot R = \partial_y \phi \quad \text{at} \quad y = R(t) \quad \text{(wavemaker)} \tag{1f}$$

$$\delta W : \dot Z = W \tag{1g}$$

$$\delta Z : M \dot W + Mg + \underline{\frac{\gamma G(Z)}{L_i}(P_Q + K(Z))} - \rho_0 \int_0 \int_{R(t)}^{l_y(x)} \lambda \Theta (y - y_b(x,t))\, xy = 0 \tag{1h}$$

$$\delta P_Q : \dot Q = (P_Q + K(Z))/L_i \equiv I, \tag{1i}$$

$$\delta Q : \dot P_Q = -(R_c + R_i) I - \frac{I n_q V_T \ln(1 + \frac{|I|}{I_{sat}})}{|I|}. \tag{1j}$$

Coupling terms have been underlined, including a term with the pressure $\lambda(x,y,t)$ on the buoy in the Bernoulli equation at the free or buoy surface, and one involving a triple integral $G(Z)$ in the buoy's momentum equation.

2. Wave-energy device

Our device consists of a contracting channel with a wave-buoy constrained to move in only one dimension, either in the vertical by sliding along a guiding mast or along a slightly curved arc pivoting around a horizontal axel at the contraction entrance. Attached to the buoy is either another vertical mast or a curved mast, to which magnets are attached that can move through a series of coils when the buoy is heaving due to the wave motion. An artistic rendering of the second version of the wave-energy device is given in Fig. 1.

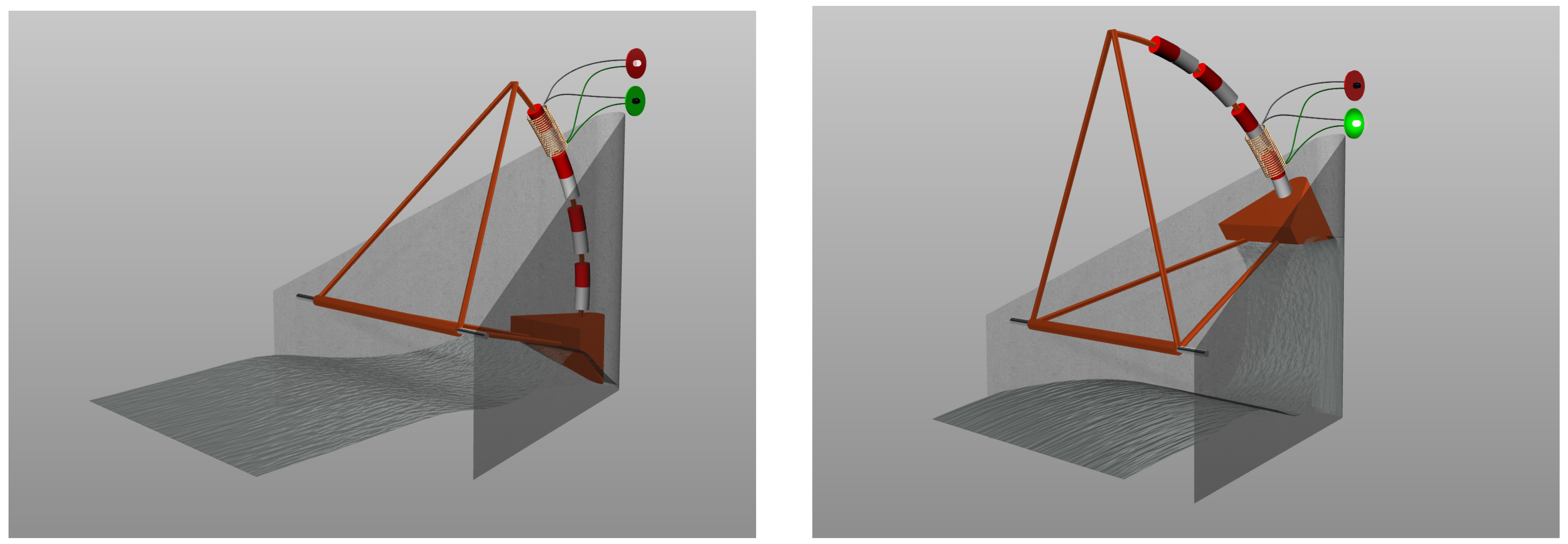

Figure 1: Sketches of our wave-energy device with its horizontal axel at the contraction entrance, its three-dimensional buoy in the contraction indicated in yellow/orange, attached to an induction motor, consisting of magnets on the arc moving through the hollow cylindrical coils indicated in yellow, as well as a green and red LED.

The latter magnet-and-coil system comprises a magnetic-induction motor, cf. the one in the Faraday shaking light shown in Fig. 2. Relative to the version with the two vertical masts, one moving and one fixed, it has the advantage that the buoy can be taken out of action in storms and that a rotating axel is mechanically more robust than mast-guide ball-bearings. Our device is intended to be part of a breakwater or dock since waves will be absorbed. For a proof-of-principle, see `https://www.youtube.com/watch?v=SZhe_SOxBWo&t=254s`

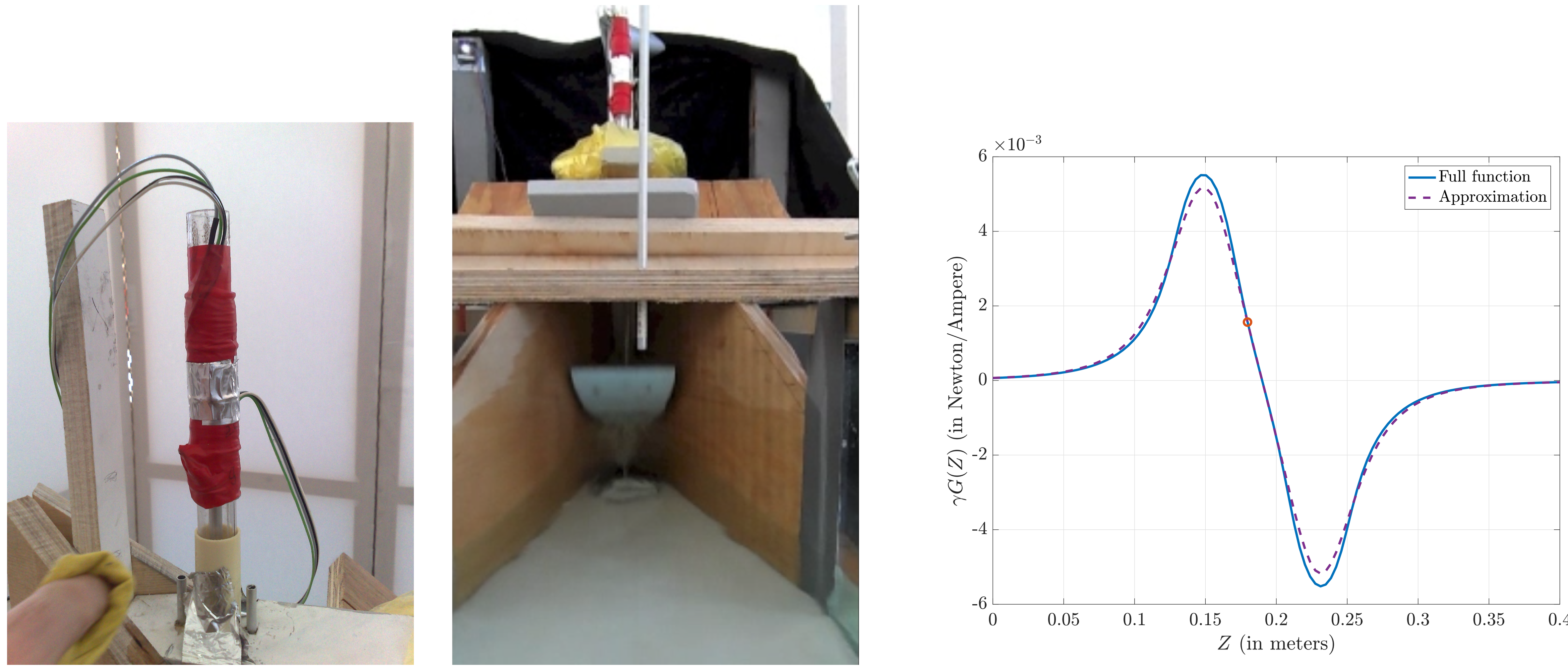

(a) (b) (c)

Figure 2: Details of our new wave-energy device: a) The magnetic-induction motor consisting of the hollow tube with its four sets of coils; a tube through which the magnets on top of the buoy-mast move; b) the blinking LED light (seen as the white flash at the top left) while the buoy is elevated by a wave to its top position; and, (c) function $G(Z)$ (derived and defined in [1,2] based on solving Maxwell's equations) and its approximation $G_{\text{approx}}(Z)$ in the far field of the magnet (defined in [2]); circle denotes the value $G(\bar Z)$ at the rest position $\bar Z = 0.18$. All figures on this poster are taken from [1,2].

4. Preliminary optimisation

After linearisation of the full 3D nonlinear model around a state of rest and application of the shallow-water approximation, we discretize the linear dynamics in a geometrically consistent and monolithic manner using a finite-element approach in space and symplectic integrators in time [1,2]. Preliminary results are found in Figs. 3 and 4.

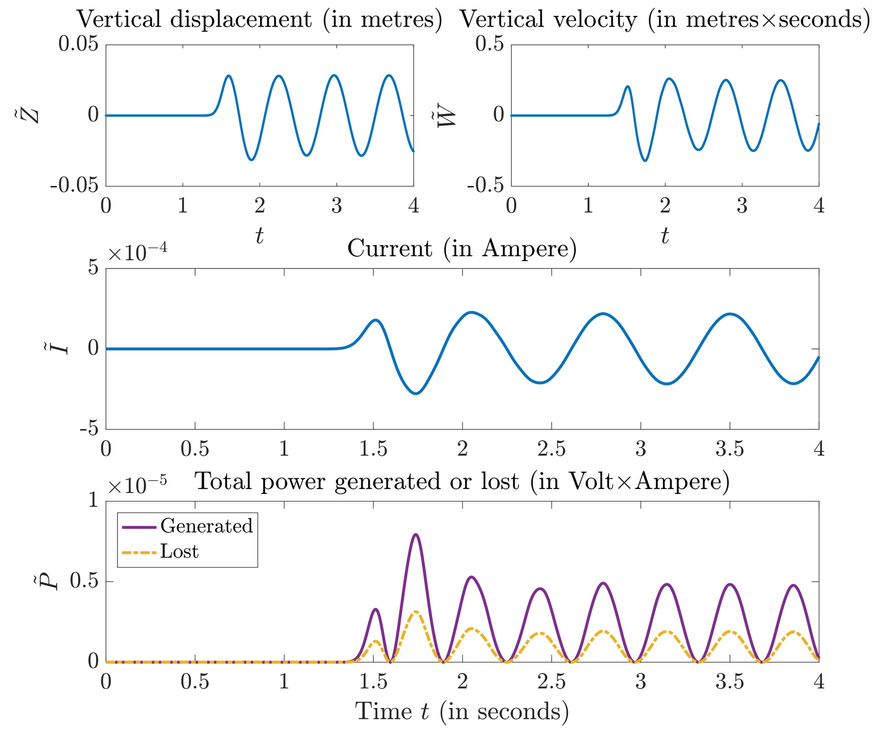

Figure 3: Output of the numerical simulation demonstrating the response of the wave-energy device to the incoming waves (panels on top row; left: vertical displacement, right: velocity). The energy generated is also shown in terms of current (middle panel) and power (bottom panel). The power output depicted in the bottom panel is divided into two parts: the power output to the LEDs (solid purple line) and the power lost in the electrical circuit (dash-dotted yellow line).

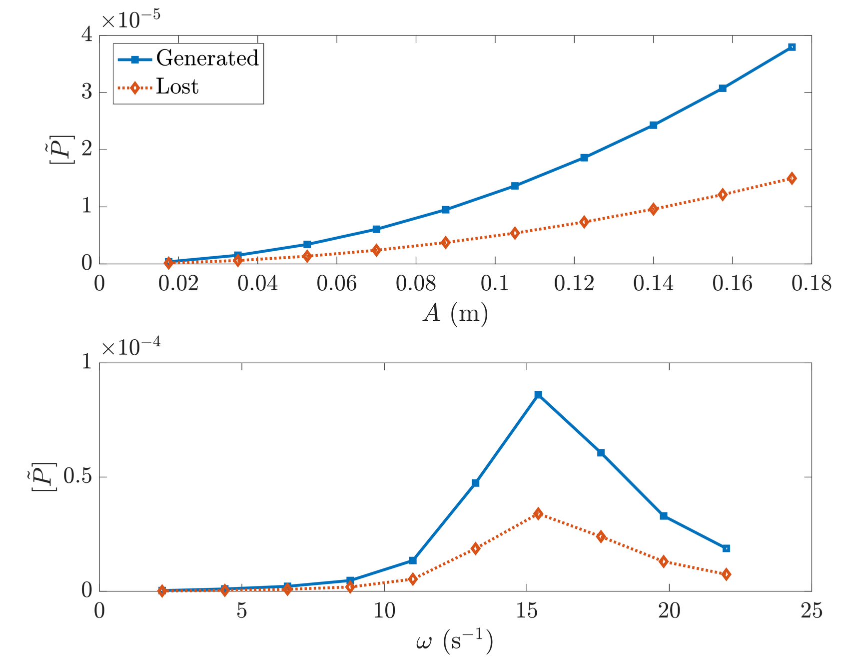

Figure 4: Variation of the total mean power generated (in Volt × Ampere) against the wavemaker amplitude or frequency. The mean power is calculated over the duration of one simulation with $T = 10$s. Top panel: varied wavemaker amplitude A (in m) with fixed frequency $\omega = 8.8\text{s}^{-1}$. Bottom panel: varied wavemaker frequency ω (in s^{-1}) with fixed amplitude $A = 0.0616$m.

5. Conclusions

- Preliminary numerical modelling and optimization of the linearised mathematical and numerical model is promising.
- Future work consists of further optimisation of the device for different geometries, regarding efficiency, and for a given wave-climate as well as probing alternative designs.

- [1] O.B, A. Kalogirou, W. Zweers 2019: From bore-soliton-splash to a new wave-to-wire wave-energy model. *Water Waves* **1**. https://link.springer.com/article/10.1007/s42286-019-00022-9
- [2] O.B., A. Kalogirou, D. Henry, G. Thomas 2020: A novel rogue-wave-energy device with wave amplification and induction actuator. *Int. Marine Energy J.* In press.